The Journal of Immunology

Mechanism of Action of Type II, Glycoengineered, Anti-CD20 Monoclonal Antibody GA101 in B-Chronic Lymphocytic Leukemia Whole Blood Assays in Comparison with Rituximab and Alemtuzumab

Luca Bologna, Elisa Gotti, Massimiliano Manganini, Alessandro Rambaldi, Tamara Intermesoli, Martino Introna and Josée Golay

J Immunol 2011; 186:3762-3769; Prepublished online 4 February 2011;
doi: 10.4049/jimmunol.1000303
http://www.jimmunol.org/content/186/6/3762

The Journal of Immunology is published twice each month by
The American Association of Immunologists, Inc.,
1451 Rockville Pike, Suite 650, Rockville, MD 20852

Print ISSN: 0022-1767 Online ISSN: 1550-6606.

Mechanism of Action of Type II, Glycoengineered, Anti-CD20 Monoclonal Antibody GA101 in B-Chronic Lymphocytic Leukemia Whole Blood Assays in Comparison with Rituximab and Alemtuzumab

Luca Bologna, Elisa Gotti, Massimiliano Manganini, Alessandro Rambaldi, Tamara Intermesoli, Martino Introna, and Josée Golay

We analyzed in B-chronic lymphocytic leukemia (B-CLL) whole blood assays the activity of therapeutic mAbs alemtuzumab, rituximab, and type II glycoengineered anti-CD20 mAb GA101. Whole blood samples were treated with Abs, and death of $CD19^+$ B-CLL was measured by flow cytometry. Alemtuzumab efficiently lysed B-CLL targets with maximal lysis at 1–4 h (62%). In contrast, rituximab induced a more limited cell death (21%) that was maximal only at 24 h. GA101 killed B-CLL targets to a similar extent but more rapidly than rituximab, with 19.2 and 23.5% cell death at 4 and 24 h, respectively, compared with 7.9 and 21.4% for rituximab. Lysis by both rituximab and GA101 correlated directly with CD20 expression levels (r^2 = 0.88 and 0.85, respectively). Interestingly, lysis by all three Abs at high concentrations was mostly complement dependent, because it was blocked by the anti-C5 Ab eculizumab by 90% in the case of alemtuzumab and rituximab and by 64% in the case of GA101. Although GA101 caused homotypic adhesion, it induced only limited (3%) direct cell death of purified B-CLL cells. Both rituximab and GA101 showed the same efficiency in phagocytosis assays, but phagocytosis was not significant in whole blood due to excess Igs. Finally, GA101 at 1–100 μg/ml induced 2- to 3-fold more efficient NK cell degranulation than rituximab in isolated B-CLL or normal PBMCs. GA101, but not rituximab, also mediated significant NK cell degranulation in whole blood samples. Thus, complement and Ab-dependent cellular cytotoxicity are believed to be the major effector mechanisms of GA101 in whole blood assays. *The Journal of Immunology*, **2011, 186: 3762–3769.**

The chimeric anti-CD20 Ab rituximab has demonstrated therapeutic activity in B non-Hodgkin's lymphomas (B-NHL) and other mature B cell neoplasias. The addition of rituximab to chemotherapy resulted in improved cure rates in diffuse large B cell NHL and overall survival benefits for patients with follicular lymphoma (FL) and B-chronic lymphocytic leukemia (B-CLL) if used as upfront treatment. Despite this high standard of care, the question remains how to improve current therapy options in B-NHL and B-CLL patients (1, 2). Indeed, even in B-NHL patients undergoing complete response to treatment, relapse remains a major problem. Furthermore, rituximab as a single agent has shown relatively limited efficacy in B-CLL and mantle cell lymphoma compared with FL. In B-CLL, rituximab has, however, significant activity at the higher dose levels (3).

Laboratory of Cellular Therapy "G. Lanzani," Division of Hematology, Ospedali Riuniti, 24128 Bergamo, Italy

Received for publication February 1, 2010. Accepted for publication January 3, 2011.

This work was supported in part by the Associazione Italiana Ricerca contro il Cancro (individual grant to J.G.) and the Associazione Italiana Lotta alle Leucemie, Linfomi e Mieloma.

Address correspondence and reprint requests to Dr. Martino Introna, Laboratory of Cellular Therapy "G. Lanzani," Division of Hematology, Ospedali Riuniti, c/o Presidio Matteo Rota, Via Garibaldi 11-13, 24128 Bergamo, Italy. E-mail address: mintrona@ospedaliriuniti.bergamo.it

The online version of this article contains supplemental material.

Abbreviations used in this article: 7-AAD, 7-aminoactinomycin D; ADCC, Ab-dependent cellular cytotoxicity; B-CLL, B-chronic lymphocytic leukemia; B-NHL, B non-Hodgkin's lymphoma; CDC, complement-dependent cytotoxicity; FL, follicular lymphoma; HS, human serum; MNC, mononucleated cell; TX, control Ab trastuzumab.

At least seven new anti-CD20 Abs have been designed with the purpose of further improving the therapeutic efficacy of rituximab and have entered clinical trials in the last 5 y (4). In comparison with rituximab, these molecules have been humanized or selected for either increased or decreased complement activation capacity, improved Ab-dependent cellular cytotoxicity (ADCC), for example, with augmented binding to the low-affinity polymorphic form of CD16A (Phe/Phe at position 158), and, in some cases, increased proapoptotic property. One such molecule is GA101, a type II glycoengineered humanized anti-CD20 Ab (5, 6), which has been reported to mediate superior ADCC and induce significant direct cell death of lymphoma cell lines in vitro (7, 8). GA101 has shown promising activity in preclinical animal models and phase I/II clinical trials in B-NHL and B-CLL (8–12).

The variety of modifications brought to the anti-CD20 mAbs presently in clinical development at least in part reflect the still incomplete knowledge about translation of preclinical findings into the clinic and the most important mechanism of action of rituximab in vivo in man, although a number of studies have been performed in vitro and several mouse models investigated (13–19). Indeed, rituximab activates complement, lyses neoplastic targets efficiently in vitro, and mediates ADCC by NK cells as well as phagocytosis by macrophages (20–22), but the relative importance of each of these mechanisms in vivo is still unclear (4, 23, 24). For FL, FcγRIIIA polymorphism analysis suggests a role of ADCC in vivo but this is unlikely to be the only mechanism (25). The most controversial aspect is the role of complement, because its activation has been variably suggested to be fundamental (14, 26), to contribute to the in vivo activity of the Ab (15, 16), to have no role, or even to be detrimental (17, 27). Finally, different

www.jimmunol.org/cgi/doi/10.4049/jimmunol.1000303

mechanisms may be predominant according to tissue localization of target B cells, levels of CD20 expression, tumor burden, or other yet undefined factors (28–30). Thus, it is crucial not only to determine the most important biological activity of the Ab in vivo, but also to establish its mode of action for each tissue/disease type.

With these problems in mind, we have set up assays that could measure the biological properties of therapeutic mAbs in unmanipulated whole blood from B-CLL patients, with the view of: 1) having a rapid assay to test the efficacy of novel Abs against B-CLL or normal B cells in the circulation; and 2) having a tool to dissect the role of different mechanisms of target cell killing by mAbs in a context as unmanipulated as possible. With this method, we have compared the efficacy and mechanism of action of alemtuzumab, rituximab, and GA101 against B-CLL cells.

Materials and Methods

Cells

Peripheral blood was drawn either in 0.1 M Na citrate vacuette tubes (BD Biosciences, San Diego, CA) or in lepirudin (Refludan; Celgene, Summit, NJ) at 500 μg/ml final concentration. Blood was obtained from patients with B-CLL, indolent B-NHL with significant circulating disease (at least 50% of neoplastic cells in the mononuclear cell fraction), or normal donors, after informed consent. All patients were diagnosed by routine immunophenotypic, morphologic, and clinical criteria. Double staining for CD19 and surface Igk or Igλ was performed to establish monoclonality and determine the percentage of neoplastic versus normal B cell present in the samples (>95%). In some cases, the mononucleated cell (MNC) fraction was also purified by standard Ficoll Hypaque gradient centrifugation (Seromed, Berlin, Germany). MNC were then cultured in Stem Span SFEM medium (StemCell Technologies, Vancouver, Canada). The study was approved by the Hospital Ethical Committee.

The DHL4 cell line has been described previously (20) and was grown in RPMI 1640 medium supplemented with 10% FCS (Euroclone; Wetherby, West Yorkshire, U.K.), 2 mM glutamine (Euroclone), and 110 μM gentamicin (PHT Pharma, Milano, Italy).

Immunofluorescence analyses

Whenever possible, the absolute number of CD20 molecules was measured on the mononucleated fraction using PE-labeled anti-CD20 and calibrated Quantibrite beads (BD Biosciences), following the manufacturer's instructions (29).

Complement-dependent cytotoxicity and complement fragment deposition

B-CLL were cultured at 4×10^5/ml in medium supplemented with 20% human serum (HS) and/or different concentrations of mAbs. For complement-dependent cytotoxicity (CDC), cells were collected after 4–24 h incubation at 37°C 5% CO_2, stained with CD19-PE and 7-aminoactinomycin D (7-AAD), and analyzed by flow cytometry using a FACScan instrument (BD Biosciences). For complement deposition measurement, after 1 h incubation at 37°C 5% CO_2, cells were washed with PBS solution and stained with the anti-C9 mAb aE11 and goat anti-mouse FITC-conjugated secondary Ab (BD Biosciences) or with Alexa 488-labeled anti-C3 mAb 1H8 specific for C3b/iC3b/C3dg (a kind gift of Prof. R. P. Taylor, University of Virginia School of Medicine, Charlottesville, VA) (31). After washing in PBS, cells were analyzed by flow cytometry.

Measurement of Ab-induced cell death in whole blood

A total of 200 μl unmanipulated peripheral blood of B-CLL/B-NHL patients in 0.1 M Na citrate solution was plated in sterile nonpyrogenic round-bottom tubes, and different concentrations of alemtuzumab, rituximab, GA101, or irrelevant control Ab trastuzumab (TX) were added. In some cases, 200 μg/ml blocking anti-C5 mAb eculizumab (Soliris; Alexion Pharmaceuticals, Cheshire, CT) or control irrelevant Ab were added 5 min before the lytic Abs. Whole blood samples were incubated for 1–24 h at 37°C and then stained for 15 min at room temperature with allophycocyanin-Cy7–conjugated anti-CD45, FITC-conjugated anti-CD19 Ab, and PerCP complex (PerCP)/7-AAD (all from BD Biosciences). After incubation, samples were lysed with hypotonic lysis solution (Pharm Lyse; BD Biosciences) to eliminate platelets and RBCs and then analyzed by double fluorescence on an FACSCanto instrument (BD Biosciences). Cell death was measured as a decrease in the $CD19^+/7\text{-}AAD^-$ population in treated versus control samples after gating on the $CD45^+$ population. In some experiments, a fixed volume of calibration beads was added to each sample before FACS analysis to measure the decrease in absolute number of $CD19^+/7\text{-}AAD^-$. The results obtained measuring relative or absolute decrease in B cells were equivalent (data not shown).

CDC and direct cell death measurement in cytospins

B-CLL mononuclear cells were cultured in Stem Span SFEM medium (Stem Cell Technology, Vancouver, British Columbia, Canada) at 4×10^5 cells/ml in the presence (CDC) or absence (direct cell death) of 20% HS and different mAbs. After 24 h at 37°C 5% CO_2, cells were stained for 15 min with 7-AAD, washed in PBS, and centrifuged onto glass slides at 500 rpm for 5 min using a Shandon centrifuge. Slides were dried, fixed in 100% methanol, and nuclei stained with 1.5 μg/ml DAPI in mounting medium (Vectashield; Vector Laboratories, Burlingame, CA). At least five representative fields were photographed under a fluorescence microscope. Total number of cells ($DAPI^+$) and percentage of dead cells ($7\text{-}AAD^+$) were then counted in a blind fashion using the ImageJ program (National Institutes of Health).

Alamar blue cytotoxicity assay

B-CLL mononuclear cells were plated at 10^5/well in Stem Span SFEM medium supplemented with 10 μg/ml mAbs. After 24 or 48 h incubation at 37°C 5% CO_2, 1/10 volume Alamar blue solution (Biosource International, Camarillo, CA) was added and incubated overnight. The plates were then read in a fluorimeter (Tecan Austria, Salzburg, Austria) with excitation at 535 nm and emission at 590 nm. Cytotoxicity was calculated as percentage of fluorescence with respect to untreated control, after subtracting for background fluorescence in absence of cells.

Phagocytosis assay

$CD14^+$ monocytes were purified from healthy volunteers' mononuclear cells by immunomagnetic sorting as previously described (21) and cultured in eight-well chamber slides (LabTek; Nunc) at 2×10^5 cells/well for 6 to 7 d in RPMI 1640 medium supplemented with 20% heat-inactivated FCS and 20 ng/ml recombinant human M-CSF (R&D Systems) to give rise to differentiated macrophages. Phagocytosis was performed by adding 2×10^5 PBMCs in 300 μl or 300 μl whole blood from B-CLL patients to the macrophages in the presence or absence of rituximab, GA101, and/or increasing concentrations of Na citrate, 20% HS, or 50 μg/ml i.v. Ig. After 2 h at 37°C, slides were gently rinsed in PBS, fixed in methanol, and stained with Giemsa. Slides were analyzed under a light microscope using a grid, counting macrophages in a double blind fashion. The percentage of phagocytosis was expressed as the percentage of macrophages that engulfed at least one tumor cell with respect to total macrophages.

Measurement of NK cell activation

MNC from normal donors or whole blood in lepirudin were treated with different concentrations of GA101, rituximab, or TX for 3 h at 37°C. Cells were then incubated with anti–CD56-allophycocyanin and anti–CD107a-PE for 20 min, washed in PBS, and, in the case of whole blood, red cells were lysed in hypotonic lysing solution as above and analyzed on an FACSCanto instrument (BD Biosciences). Cells were gated on the mononuclear population, and the percentage of CD107a in the $CD56^+$ fraction was then measured. The results are expressed as the percentages of CD107a expression on $CD56^+$ cells in treated samples after subtracting the background of TX-treated controls. Double staining of the control samples with anti–CD56-allophycocyanin and anti–CD16-FITC demonstrated that in all cases, >95% of $CD56^+$ cells were $CD16^+$ NK cells.

Statistical analysis

The data were analyzed using the paired or unpaired Student *t* test, as appropriate: $*p < 0.05$, $**p < 0.01$, $***p < 0.001$.

Results

Lysis of B-CLL cells in whole blood by alemtuzumab is complement dependent

To measure the activity of therapeutic mAbs in vitro in conditions as physiological as possible, we have tested several standard anticoagulants to exclude that they may interfere with effector mechanisms of therapeutic mAbs in vitro. We initially used the anti-CD52 Ab alemtuzumab and anti-CD20 Ab rituximab as test Abs, because their immune-mediated mechanisms on purified B-

CLL cells are well characterized (32, 33). We observed that Na citrate solution from vacutainer tubes, at the standard concentration used for anticoagulant activity (0.1 M), did not inhibit either complement activation induced by alemtuzumab in presence of 20% HS, measured as C3 and C9 deposition (Fig. 1*A*), or cell lysis (Fig. 1*B*). Furthermore, 0.1 M citrate did not inhibit significantly rituximab-mediated phagocytosis (Fig. 1*C*).

We therefore used freshly isolated B-CLL whole blood samples drawn in Na citrate solution to investigate the cytotoxic activity of alemtuzumab. As shown in Fig. 2*A*, at 10 μg/ml and after 4 h, this Ab killed the B-CLL targets somewhat less efficiently in whole blood compared with purified cells in presence of 20% HS, with a mean 50% lysis in whole blood compared with 80% of purified cells in 20% HS ($p < 0.01$). Alemtuzumab-induced cell death was dose and time dependent with maximal lysis observed already at 1 h at 25 μg/ml Ab (Fig. 2*B* and data not shown). Control Ab TX had no effect (data not shown). We then wished to determine the role of complement in the efficacy of alemtuzumab in whole blood assays. For this purpose, we incubated the cells with excess blocking anti-C5 Ab eculizumab (200 μg/ml) (34) and then added 10 μg/ml alemtuzumab. As shown in Fig. 2*C*, target cell killing by anti-CD52 was essentially abolished by excess eculizumab at both 4 and 24 h. Study of C3 and C9 deposition on mononuclear cells in whole blood in the presence or absence of alemtuzumab and/or eculizumab confirmed that alemtuzumab induced rapid deposition of both C3 and C9 in absence of eculizumab. Furthermore, the anti-C5 Ab blocked C9 but not C3 deposition, as expected (Fig. 2*D*).

We conclude that alemtuzumab rapidly lyses B-CLL targets in whole blood by a complement-dependent mechanism.

Lysis of B-CLL targets in whole blood by rituximab and GA101

We next investigated the activity of the anti-CD20 Ab rituximab in whole blood. For most B-CLL samples, rituximab was much less effective than alemtuzumab in inducing cell lysis, with a mean 12 and 15% lysis after 24 h in presence of 10 or 200 μg/ml anti-CD20 Ab, respectively, compared with 77% with 10 μg/ml alemtuzumab

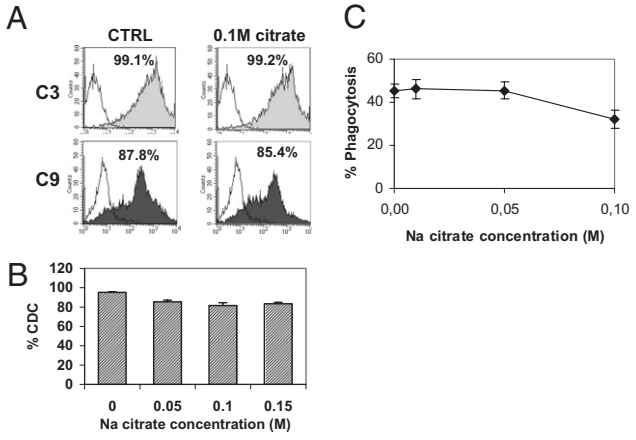

FIGURE 1. Na citrate does not inhibit significantly CDC or phagocytosis. *A* and *B*, Mononuclear cells from B-CLL patients were incubated with 10 μg/ml alemtuzumab and 20% HS in presence of increasing concentrations of Na citrate solution. Deposition of C3 and C9 was measured after 1 h incubation by direct and indirect immunofluorescence, respectively (*A*), and percentage cell death was measured after 4 h by 7-AAD staining and FACS analysis (*B*). *C*, Phagocytosis assays were performed with macrophages, B-CLL, and 10 μg/ml rituximab in culture medium in presence of increasing concentrations of Na citrate solution. All results are the mean and SD of duplicate wells and are representative of two experiments.

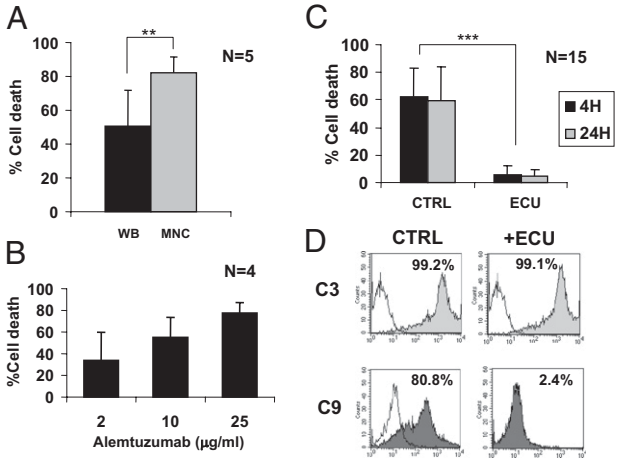

FIGURE 2. Alemtuzumab kills B-CLL cells in whole blood (WB) through complement. Either WB from B-CLL patients in 0.1 M Na citrate solution (*A–C*) or MNC in culture medium + 20% HS (*A*) were incubated with 10 μg/ml or the indicated concentrations of alemtuzumab, in presence or absence of 200 μg/ml eculizumab (ECU). Incubation times were 4 h unless otherwise indicated. Percentage cell death was measured as a decrease in $CD19^+/7\text{-}AAD^-$ cells relative to untreated control (*A–C*). C3 and C9 deposition was measured by direct and indirect immunofluorescence, respectively (*D*). $^{**}p < 0.01$, $^{***}p < 0.001$.

($p < 0.001$). Thus, in vitro, the dose of 200 μg/ml rituximab was not significantly more effective in lysing B-CLL cells than that of 10 μg/ml (Fig. 3*A*). Time course experiments showed that, in 12 experiments, mean lysis with alemtuzumab was already maximal at 4 h (62%), whereas that induced by rituximab was higher at 24 h (21%) compared with 4 h (7.8%) ($p > 0.001$; Fig. 3*B*).

GA101 is a type II, glycoengineered, anti-CD20 Ab that has recently entered clinical trials (5). We therefore compared the effect of rituximab and GA101 on B-CLL cells in whole blood assays. Doses of 100 μg/ml were used because these levels and above are reached in vivo. Whereas rituximab required 24 h for maximal lysis (mean 21.4%, $n = 17$), the effect of GA101 on the samples was more rapid, with near maximal cell death observed already at 4 h (19.2%), which increased a little further at 24 h (23.5%)(Fig. 4*A*). Lysis by both rituximab and GA101 correlated

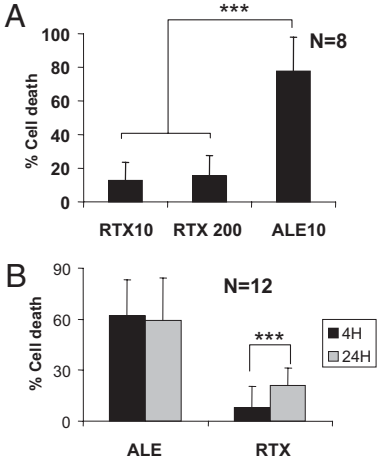

FIGURE 3. Rituximab (RTX) lyses B-CLL samples less efficiently than alemtuzumab (ALE). ALE or RTX at 10 μg/ml (*A*, *B*) and RTX at 200 μg/ml (*A*) were added to whole blood from B-CLL patients for 24 h (*A*) or both 4 (black bars) and 24 h (gray bars) (*B*) and percentage cell death of neoplastic B cells measured by FACS analysis. The results are the means and SD of 8–12 different samples analyzed, as indicated. $^{***}p < 0.001$.

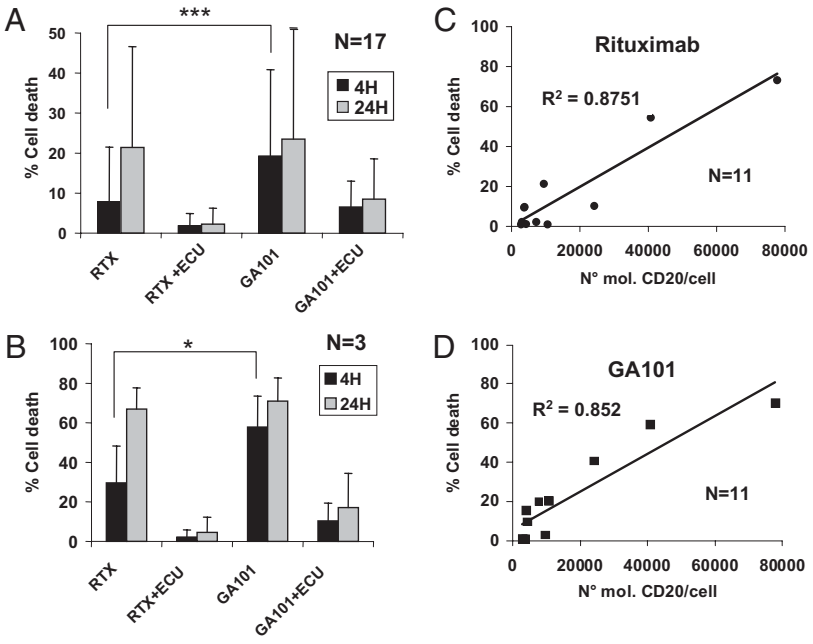

FIGURE 4. Activities of RTX and GA101 in whole blood assays. *A* and *B*, RTX or GA101 were added to B-CLL/B-NHL whole blood samples at 100 μg/ml and percentage cell death of neoplastic B cell targets measured by FACS analysis after 4 (black bars) and 24 h (gray bars). In some cases, 200 μg/ml eculizumab (ECU) was also added as indicated. Seventeen random B-CLL samples were used in *A*, whereas three B-CLL/B-NHL samples selected for high expression levels of CD20 were used in *B*. Percentages of cell death with 100 μg/ml RTX (*C*) or GA101 (*D*) at 24 h were plotted against CD20 expression levels, measured as number of CD20 molecules/cell, and r^2 calculated. *$p < 0.05$, ***$p < 0.001$.

with CD20 expression levels (Fig. 4*C*, 4*D*, respectively). Finally, when three samples selected for high CD20 levels were analyzed, the difference between rituximab and GA101 at 4 h was still significant, with a mean 57.9% killing with GA101 compared with 29.5% with rituximab ($p < 0.05$; Fig. 4*B*).

We next determined the role of complement in anti-CD20 mAb-induced lysis. Addition of eculizumab to the test tubes showed that rituximab-mediated killing is mostly complement dependent because cell death was inhibited by ~90% at 24 h after blocking C5 activation (Fig. 4*A*). Surprisingly, GA101-mediated killing at 100 μg/ml was also strongly, although not completely, dependent upon complement, with a mean 64% inhibition of killing by eculizumab at the same time point (Fig. 4*A*). Similar data were obtained with the selected patient samples expressing high levels of CD20 (n = 3; Fig. 4*B*).

We wondered whether the 6–16% residual cell death induced by GA101, which was not inhibited by eculizumab, may have been due to direct cell death, as previously suggested for other type II anti-CD20 mAbs (35). We therefore further analyzed this phenomenon using purified mononuclear cells from B-CLL samples. In these conditions, we first noticed that GA101 induced strong homotypic adhesion of most B lymphoma cell lines (7 and data not shown) and, to a lesser and variable extent, of B-CLL samples (Fig. 5*A*). Because we had previously demonstrated that direct cell death can be dramatically misinterpreted by flow cytometry when using Abs that cause cell aggregation (36), we chose to further investigate possible direct cell death induction using the vital dye Alamar blue (Biosource International) and purified B-CLL mononuclear cells. As shown in Fig. 5*B*, 100 μg/ml GA101 or rituximab induced <5% direct cell death of B-CLL cells compared with TX, after either 24 or 48 h incubation. The same results were obtained using 10 μg/ml Abs (data not shown). To confirm this finding using a different method, MNC from B-CLL patients were treated with 10 μg/ml Abs for 24 h, stained with 7-AAD, and centrifuged onto glass slides. The cytospin preparations were then fixed and counterstained with DAPI. Percentages of 7-AAD$^+$ cells with respect to total number of cells (DAPI$^+$) were then counted under the microscope. The data show that, in the absence of HS, ~3% increased direct cell death could be observed with GA101, but not rituximab, with respect to control (Fig. 5*C*). This increase was very small but statistically significant. As expected, in the presence of serum, up to 70% lysis of neoplastic B cell samples expressing high levels of CD20 could be measured following treatment of the MNC with 100 μg/ml rituximab or GA101, and this lysis was completely blocked by eculizumab (Fig. 5*D*, *left panel*). In contrast, low CD20 samples were poorly lysed in presence of HS (Fig. 5*D*, *right panel*). These data confirm using cytospins that complement is the major mechanism of lysis of B-CLL cells in presence of anti-C20 mAbs and serum and is dependent upon CD20 expression levels.

The major role of complement with GA101 was surprising because this Ab is known to be less effective at binding C1q and activating complement (7). We therefore performed a standard CDC assay using a B lymphoma cells line with rituximab and GA101 in parallel. We indeed observed that GA101 was less active that rituximab at low doses in this assay, but that CDC was equivalent with both Abs at the 10 μg/ml dose and above (Supplemental Fig. 1 and data not shown). Finally, we performed dose-response curves with GA101 Ab in B-CLL whole blood assays in the presence and absence of eculizumab. We observed a rapid decrease in CDC using 10 μg/ml and 1 μg/ml GA101 in whole blood compared with the 100 μg/ml dose (data not shown). This is in agreement with the fact that relatively high doses of GA101 are required for efficient CDC in vitro (Supplemental Fig. 1*C*).

Altogether, these data suggest that lysis of B-CLL cells induced by 100 μg/ml rituximab or GA101 in whole blood is mostly due to complement activation and is dependent on CD20 expression levels. GA101, but not rituximab, induces homotypic adhesion of B-CLL and a very small increase in direct cell death.

Both GA101 and rituximab induce phagocytosis, but this is inhibited by excess Igs

To further investigate whether the residual, complement-independent cell death induced by GA101 in whole blood assays may be due to phagocytosis, we next compared the activity of rituximab and GA101 in phagocytosis assays using in vitro-differentiated macrophages and purified B-CLL cells as targets. As shown in Fig. 6*A*, both rituximab and GA101 showed overlapping dose-response curves in standard phagocytosis assays in culture medium, suggesting similar efficacy of the two Abs

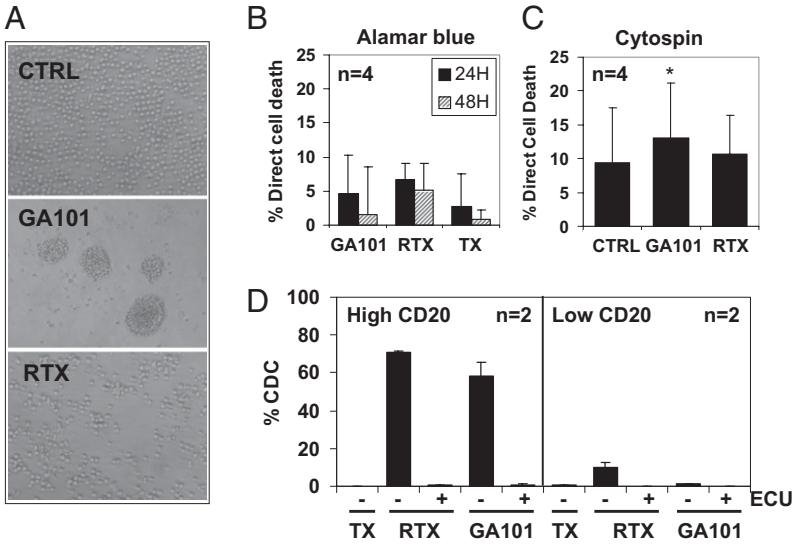

FIGURE 5. GA101 induces homotypic adhesion of B-CLL cells but little increase in direct cell death. *A*, Total of 10 μg/ml GA101 or RTX were added to B-CLL MNC and homotypic adhesion observed under the microscope after 24 h. The pictures are representative of four experiments performed in duplicate. *B*, B-CLL MNC were cultured for 24 (black bars) or 48 h (gray bars) in presence of 100 μg/ml GA101, RTX, or TX and percentage cell death measured with the Alamar blue dye. *C*, B-CLL MNC were cultured for 24 h in presence of 10 μg/ml indicated Abs, stained with 7-AAD, and cytopins counterstained with DAPI. Percentage of 7-AAD$^+$/DAPI$^+$ dead cells was then scored. The results of *B* and *C* are the means and SD of four experiments. *D*, B-CLL MNC expressing either high CD20 (*left panel*) or low CD20 (*right panel*) were incubated with 100 μg/ml RTX, GA101, or TX in presence or absence of 200 μg/ml eculizumab. After 24 h, 7-AAD was added, and cells were cytospinned, fixed, and counterstained with DAPI. Percentage 7-AAD$^+$DAPI$^+$ dead cells was then evaluated under the microscope. *$p < 0.05$.

through this mechanism. We then investigated whether phagocytosis could take place in whole blood. We observed that neither rituximab nor GA101 were able to mediate significant phagocytosis in whole blood (Fig. 6*B* and data not shown). Inhibition was probably due to the presence of high amounts of IgGs in whole blood because phagocytosis mediated by rituximab in culture medium was strongly inhibited in presence of either 20% HS or excess Igs (50 μg/ml; Fig. 6*B*) (21).

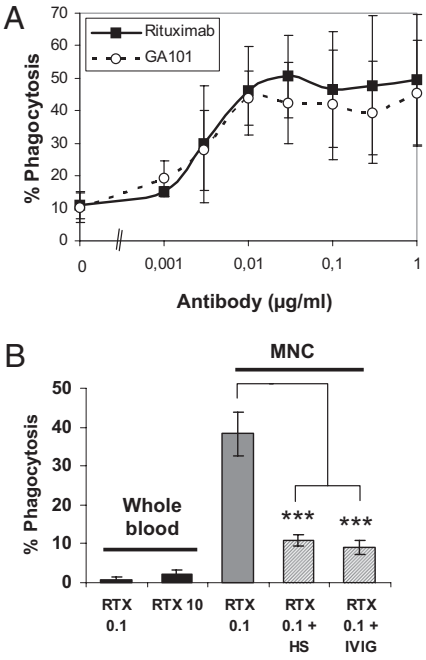

FIGURE 6. Both GA101 and RTX mediate phagocytosis, but not in whole blood. *A*, Phagocytosis assays were performed with macrophages and B-CLL in culture medium in presence of increasing concentrations of either RTX or GA101. The results are the means and SD of three experiments. *B*, Phagocytosis assays were performed with B-CLL in whole blood or MNC from B-CLL patients in presence of 0.1 or 10 μg/ml RTX and either 20% HS or 50 μg/ml i.v. Ig. The results are the mean and SE of duplicate wells and are representative of three independent experiments. ***$p < 0.001$.

We conclude that GA101 and rituximab are equally potent in mediating phagocytosis, but that this mechanism is not likely to contribute significantly to target cell killing in whole blood.

GA101 is more effective than rituximab at activating NK cells in whole blood

Using B lymphoma cell lines as targets, GA101 has been previously demonstrated to bind more tightly to the FcγRIII receptor (CD16) than rituximab and to induce higher ADCC (7). To investigate the possible contribution of ADCC in B-CLL whole blood, we searched for surrogate markers of NK cell activation that could be used in this context. Up to 50% CD107a induction and 90% CD16 downmodulation on CD56$^+$ NK cells could be measured at 2 and 24 h, respectively, following addition of anti-CD20 Abs to MNC from either normal donors or B-CLL patients (Fig. 7*A* and data not shown). However, CD107a, a marker of degranulation, was more reproducible and correlated better with target cell lysis with respect to CD16 downmodulation (data not shown). We therefore chose to use CD107a induction as a surrogate marker of ADCC in whole blood. We observed, however, that citrate strongly inhibited degranulation in MNC samples and therefore searched for other anticoagulants. We found that, in contrast, the leech-derived molecule lepirudin had no effect on CD107a degranulation (Fig. 7*B*). We therefore used lepirudin-treated whole blood to measure NK cell activation. CD107a was induced up to 7 and 19.5% on NK cells in the blood from normal donors and B-CLL patients, respectively, following addition of 1–100 μg/ml GA101 Ab (Fig. 7*C*, 7*D*). In contrast, an increase of <1% CD107a expression was observed following addition of the same doses of rituximab (Fig. 7*C*, 7*D*).

We finally verified whether lepirudin modified the cell death data measured in whole blood assays compared with citrate. Using two B-CLL whole blood samples in lepirudin, we observed 20% cell death in presence of 100 μg/ml GA101 after 4 h exposure compared with 10% for rituximab (data not shown). A total of 79 and 90% of this lysis was blocked by eculizumab, respectively. These data are very similar to those observed in citrate (Fig. 4*A*) and confirm a higher cell death induced by GA101 at 4 h and a major contribution of complement for both rituximab and GA101 in these conditions.

We conclude that NK cells are activated in whole blood by GA101 more efficiently than by rituximab and that this mechanism

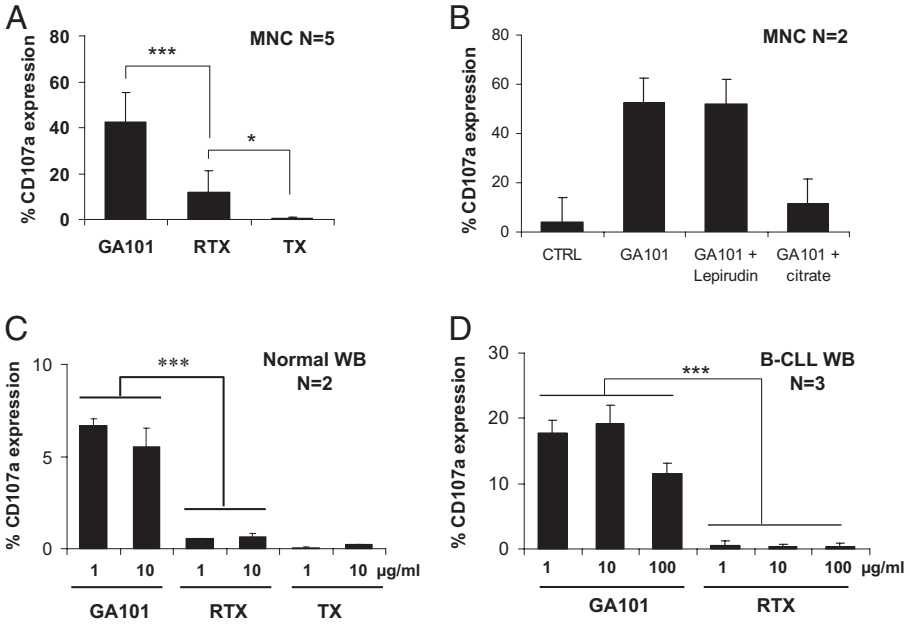

FIGURE 7. GA101 but not RTX induces CD107a on NK cells in normal and B-CLL whole blood. *A*, MNC from five normal donors were incubated for 3 h with 10 μg/ml GA101, RTX, or TX and percentage of CD107a expression on $CD56^+$ NK cells analyzed by flow cytometry. *B*, MNC from three normal donors were incubated for 2 h with 10 μg/ml GA101 in presence or absence of 0.1 M Na citrate or 500 μg/ml lepirudin. Percentage of CD107a expression on $CD56^+$ cells was then analyzed by flow cytometry. *C*, Total of 1 or 10 μg/ml GA101, RTX, or TX was added to lepirudin-treated whole blood (WB) from two normal donors and percentage CD107a induction on NK cells was analyzed by flow cytometry 3 h later. *D*, Total of 1, 10, or 100 μg/ml GA101 or RTX were added to lepirudin-treated WB from three B-CLL patients and percentage of CD107a induction on NK cells analyzed after 3 h. The results are the means and SD of the indicated number of experiments. $*p < 0.05$, $***p < 0.001$.

may contribute to the complement-independent cytotoxic activity of the former anti-CD20 mAb against B-CLL cells.

Discussion

In this report, we have set up novel whole blood assays to study the mechanism of action of therapeutic mAbs for circulating neoplastic B cells such as B-CLL and B-NHL, in conditions as physiological as possible. As test Ab, we used anti-CD52 mAb alemtuzumab, showing that this Ab has strong activity in whole blood with up to 77% killing of B-CLL targets in only 1–4 h using Ab concentrations that are reached in vivo (37). Furthermore, we showed, by preincubating with excess blocking anti-C5 Ab eculizumab (34), that this effect is entirely complement dependent. Indeed, cell death as well as membrane attack complex formation, but not C3 activation, was confirmed to be strongly inhibited by eculizumab in whole blood. This overwhelming role of complement in alemtuzumab-mediated killing in whole blood has not been reported previously.

The efficacy and mechanisms of action of anti-CD20 mAbs rituximab and GA101 were then analyzed. Rituximab was relatively poor at killing B-CLL cells in vitro compared with alemtuzumab, with a mean 21% lysis reached after 24 h. Also, target cell killing by rituximab was less efficient and showed slower kinetics in whole blood compared with purified neoplastic cells cultured in medium supplemented with 20% HS. The slower kinetics were likely due to inhibition of complement activation by cell-bound or fluid-phase complement inhibitors present in whole blood. Indeed, we showed that rituximab-mediated cell death was mostly due to complement, because it was inhibited to 90% by eculizumab. Furthermore, we did observe increased target cell lysis with rituximab in whole blood in presence of blocking anti-CD55 and CD59 Abs (J. Golay and M. Manganini, unpublished observations). In contrast, significant direct cell death did not take place with this Ab under the chosen conditions, and phagocytosis was relatively ineffective in whole blood, presumably due to the high concentrations of IgG present in the fluid phase that competes for FcγRs (21). Finally, ADCC was unlikely to play a role in for rituximab in this setting, because we could not detect significant CD107a induction, a marker of NK cell degranulation, in rituximab- treated whole blood samples (38). This was probably due to complement activation, which is known to inhibit rituximab-mediated NK cell activation (39).

The data obtained with eculizumab on the role of C5 complement fragment in the mechanism of action of rituximab in whole blood are of interest for several reasons: 1) they were observed in unmanipulated blood that should best mimic the events taking place in the circulation; 2) they suggest that complement acts through the membrane attack complex to induce direct target cell lysis and that killing is not mediated, for example, by immune cells recognizing deposited C3b; and 3) they demonstrate that CDC is important for the mechanism of action of rituximab in the circulation, in contrast to previous reports indicating complement to be the cause of the Ab early toxicity rather than efficacy in vivo (40). Our data are in agreement with studies suggesting complement is a limiting factor in B-CLL patients treated with rituximab (41) and that infusion of fresh-frozen plasma to patients in addition to the Ab may improve clinical response dramatically (42, 43). Our data thus suggest a significant role of complement in vivo at least for the clearance of circulating neoplastic B cells by rituximab. In contrast, clearance of neoplastic cells in tissues may require additional mechanisms, as suggested in some murine models (17, 28).

We then compared the mechanism of action of the type II anti-CD20 Ab GA101 and rituximab in whole blood assays. For both Abs, target cell killing correlated with CD20 expression levels, but GA101 had an apparently more rapid action than rituximab, with maximal cell death observed at 4 h compared with 24 h for rituximab. Also, in this case, complement appeared to be an important mechanism, because eculizumab blocked ~64% of target cell killing induced by GA101 Ab at 100 μg/ml. As expected, CDC induction by GA101 in whole blood was dose dependent and rapidly decreased at the 10 and 1 μg/ml doses. This is important information for dosing schedules in vivo.

We then also analyzed the possible mechanism of complement-independent cell killing that accounts for the residual 6–16% cell death observed in presence of eculizumab. To do this, we used purified mononuclear cells from B-CLL patients. We could show that GA101 induces homotypic adhesion of B-CLL after 4–24 h incubation, in agreement with published data (44). To avoid pos-

sible artifacts that may result from analysis of aggregated cells by flow cytometry (36), we used Alamar blue and cytospin preparations of 7-AAD–stained cells to measure direct cell death. With these methods, we could show that GA101 induces only minimal cell death (up to 3% over controls) that could be detected in cytospins. These results are in contrast with published data indicating strong direct cell death induction by GA101 in B-lymphoma cell lines (7). Our different result may be due to the target cell type analyzed in this study, B-CLL cells from patients, or the methods used. We of course cannot exclude that direct cell death by GA101 may be higher in whole blood or in longer assays.

We also investigated the possible contribution of phagocytosis to anti-CD20–mediated target cell killing using both purified B-CLL or whole blood and in vitro-differentiated macrophages. Both rituximab and GA101 showed overlapping dose-response curves with purified B-CLL cells as targets. Because the glycosylation pattern of GA101 is known to enhance binding to FcγRIIIA, these data suggest that this receptor is not the only or major receptor involved in phagocytosis mediated by these therapeutic mAbs. Indeed, we previously reported that in vitro-differentiated macrophages express high levels of FcγRI and FcγRIIA and lower amounts of FcγRIIIA (21), all of which may participate in phagocytosis. Our data are comparable to what has been described for defucosylated anti-carcinoembryonic Ag Ab, which, compared with unmodified Ab, showed enhanced ADCC but not phagocytosis (45). In contrast, phagocytosis of B-CLL in whole blood was not significant, presumably due to inhibition by serum Igs. These data suggest that phagocytosis is not a relevant mechanism of action of GA101 or rituximab in whole blood and does not explain the residual complement-independent cell killing.

Finally, a possible contribution of NK-mediated ADCC was analyzed in whole blood using CD107a induction and a surrogate marker of ADCC. In this case, we had to use lepirudin as an anticoagulant because citrate was inhibitory. We first demonstrated, using mononuclear cells from normal donors or B-CLL patients, that GA101 induces two to three times more NK cell activation than rituximab at all Ab doses. This property is presumably due to the high-affinity binding of the glycoengineered Ab to FcγRIIIa molecule (7). Furthermore, we observed significant CD107a induction by GA101, but not rituximab, on NK cells in whole blood samples from normal donors or B-CLL patients. In contrast to CDC, NK cell activation in whole blood was observed equally well with the 1 or 10 μg/ml doses of Ab. Altogether, these data strongly suggest that ADCC contributes to target cell killing by GA101 in whole blood, because CD107a is a marker of NK cell degranulation and therefore accompanies target cell killing. It was not, however, possible to formally prove this point. In any case, our results confirm the higher potency of GA101 compared with rituximab in activating NK cells in physiological conditions, a property that may also be significant in vivo.

In summary, the simple and rapid whole blood assays presented in this study to measure the activity of therapeutic mAbs in the circulation should be a useful adjunct to screen novel Abs directed at B-CLL and determine their mechanism of action in the circulation. Our data point to a major role of complement for all three mAbs analyzed, including GA101 at 100 μg/ml. GA101 in addition may induce direct cell death of B-CLL cells, but only to a very limited extent, and strongly activates NK cell degranulation in whole blood even at low Ab doses (1 μg/ml). The relevance of these findings for the mode of action in B-CLL needs to be proven by additional studies. Furthermore, whether these properties of GA101 will result in higher clinical efficacy of GA101 in vivo compared with rituximab will have to await controlled clinical studies.

Acknowledgments

We thank Dr. Christian Klein (Roche Glycart AG, Schlieren, Switzerland) for providing GA101, Prof. Ronald P. Taylor (Virginia University Medical School, Charlottesville, VA) for the gift of anti-C3 Abs and useful suggestions, Prof. A. Vannucchi (Ospedale Careggi, Firenze, Italy) for the kind gift of eculizumab, and Prof. F. Tedesco (Università degli Studi, Trieste, Italy) for providing useful advice and reagents.

Disclosures

J.G. has received grant support and honoraria from Roche Italia in the last 5 years.

References

1. Cheson, B. D., and J. P. Leonard. 2008. Monoclonal antibody therapy for B-cell non-Hodgkin's lymphoma. *N. Engl. J. Med.* 359: 613–626.
2. Gisselbrecht, C. 2008. Use of rituximab in diffuse large B-cell lymphoma in the salvage setting. *Br. J. Haematol.* 143: 607–621.
3. O'Brien, S. M., H. Kantarjian, D. A. Thomas, F. J. Giles, E. J. Freireich, J. Cortes, S. Lerner, and M. J. Keating. 2001. Rituximab dose-escalation trial in chronic lymphocytic leukemia. *J. Clin. Oncol.* 19: 2165–2170.
4. Lim, S. H., S. A. Beers, R. R. French, P. W. Johnson, M. J. Glennie, and M. S. Cragg. 2010. Anti-CD20 monoclonal antibodies: historical and future perspectives. *Haematologica* 95: 135–143.
5. Umana, P., E. Moessner, and P. Bruenker. 2006. Novel 3rd generation humanized type II CD20 antibody with glycoengineered Fc and modified elbow hinge for enhanced ADCC and superior apoptosis induction. *ASH Ann. Meeting Abs.* 108: 229.
6. Umaña, P., J. Jean-Mairet, R. Moudry, H. Amstutz, and J. E. Bailey. 1999. Engineered glycoforms of an antineuroblastoma IgG1 with optimized antibody-dependent cellular cytotoxic activity. *Nat. Biotechnol.* 17: 176–180.
7. Mössner, E., P. Brünker, S. Moser, U. Püntener, C. Schmidt, S. Herter, R. Grau, C. Gerdes, A. Nopora, E. van Puijenbroek, et al. 2010. Increasing the efficacy of CD20 antibody therapy through the engineering of a new type II anti-CD20 antibody with enhanced direct and immune effector cell-mediated B-cell cytotoxicity. *Blood* 115: 4393–4402.
8. Robak, T. 2009. GA-101, a third-generation, humanized and glyco-engineered anti-CD20 mAb for the treatment of B-cell lymphoid malignancies. *Curr. Opin. Investig. Drugs* 10: 588–596.
9. Salles, G., F. Morschhauser, T. Lamy, N. Milpied, C. Thieblemont, H. Tilly, G. Bieska, D. Carlile, and G. Cartron. 2009. Phase I study of RO5072759 (GA-101) in patients with relapsed/refractory CD20+ Non Hodgkin's Lymphoma (NHL). *ASH Ann. Meeting Abs.* 114: 679.
10. Morschhauser, F., G. Cartron, T. Lamy, N. Milpied, C. Thieblemont, H. Tilly, M. Weisser, J. Birkett, and G. Salles. 2009. Phase I study of RO5072759 (GA101) in relapsed/refractory CLL. *ASH Ann. Meeting Abs.* 114: 364.
11. Sehn, L. H., S. A. Assouline, D. A. Stewart, J. Mangel, P. Pisa, J. Kothari, and M. Crump. 2009. A Phase I study of GA101 (RO5072759) monotherapy followed by maintenance in patients with multiply relapsed/refractory CD20+ malignant disease. *ASH Ann. Meeting Abs.* 114: 385.
12. Salles, G., F. Morschhauser, C. Thieblemont, P. Solal-Celigny, T. Lamy, H. Tilly, P. Feugier, S. Le Gouill, E. Gyan, R. Bouabdallah, et al. 2010. Promising efficacy with the new anti-CD20 antibody GA101 in heavily pre-treated patients - first results from a phase II study in patients with relapsed/refractory indolent NHL (INHL). Program and abstracts of the 2010 Annual Meeting of the European Hematology Association; June 10–13, 2010; Barcelona, Spain. Abstract 0558.
13. Clynes, R. A., T. L. Towers, L. G. Presta, and J. V. Ravetch. 2000. Inhibitory Fc receptors modulate in vivo cytoxicity against tumor targets. *Nat. Med.* 6: 443–446.
14. Di Gaetano, N., E. Cittera, R. Nota, A. Vecchi, V. Grieco, E. Scanziani, M. Botto, M. Introna, and J. Golay. 2003. Complement activation determines the therapeutic activity of rituximab in vivo. *J. Immunol.* 171: 1581–1587.
15. Cragg, M. S., and M. Glennie. 2004. Antibody specificity controls in vivo effector mechanisms of anti-CD20 reagents. *Blood* 103: 2738–2743.
16. Cittera, E., M. Leidi, C. Buracchi, F. Pasqualini, S. Sozzani, A. Vecchi, J. D. Waterfield, M. Introna, and J. Golay. 2007. The CCL3 family of chemokines and innate immunity cooperate in vivo in the eradication of an established lymphoma xenograft by rituximab. *J. Immunol.* 178: 6616–6623.
17. Uchida, J., Y. Hamaguchi, J. A. Oliver, J. V. Ravetch, J. C. Poe, K. M. Haas, and T. F. Tedder. 2004. The innate mononuclear phagocyte network depletes B lymphocytes through Fc receptor-dependent mechanisms during anti-CD20 antibody immunotherapy. *J. Exp. Med.* 199: 1659–1669.
18. Hernandez-Ilizaliturri, F. J., V. Jupudy, J. Ostberg, E. Oflazoglu, A. Huberman, E. Repasky, and M. S. Czuczman. 2003. Neutrophils contribute to the biological antitumor activity of rituximab in a non-Hodgkin's lymphoma severe combined immunodeficiency mouse model. *Clin. Cancer Res.* 9: 5866–5873.
19. Minard-Colin, V., Y. Xiu, J. C. Poe, M. Horikawa, C. M. Magro, Y. Hamaguchi, K. M. Haas, and T. F. Tedder. 2008. Lymphoma depletion during CD20 immunotherapy in mice is mediated by macrophage FcgammaRI, FcgammaRIII, and FcgammaRIV. *Blood* 112: 1205–1213.
20. Golay, J., L. Zaffaroni, T. Vaccari, M. Lazzari, G. M. Borleri, S. Bernasconi, F. Tedesco, A. Rambaldi, and M. Introna. 2000. Biologic response of B

lymphoma cells to anti-CD20 monoclonal antibody rituximab in vitro: CD55 and CD59 regulate complement-mediated cell lysis. *Blood* 95: 3900–3908.
21. Leidi, M., E. Gotti, L. Bologna, E. Miranda, M. Rimoldi, A. Sica, M. Roncalli, G. A. Palumbo, M. Introna, and J. Golay. 2009. M2 macrophages phagocytose rituximab-opsonized leukemic targets more efficiently than m1 cells in vitro. *J. Immunol.* 182: 4415–4422.
22. Dall'Ozzo, S., S. Tartas, G. Paintaud, G. Cartron, P. Colombat, P. Bardos, H. Watier, and G. Thibault. 2004. Rituximab-dependent cytotoxicity by natural killer cells: influence of FCGR3A polymorphism on the concentration-effect relationship. *Cancer Res.* 64: 4664–4669.
23. Cartron, G., H. Watier, J. Golay, and P. Solal-Celigny. 2004. From the bench to the bedside: ways to improve rituximab efficacy. *Blood* 104: 2635–2642.
24. Taylor, R. P., and M. A. Lindorfer. 2008. Immunotherapeutic mechanisms of anti-CD20 monoclonal antibodies. *Curr. Opin. Immunol.* 20: 444–449.
25. Cartron, G., L. Dacheux, G. Salles, P. Solal-Celigny, P. Bardos, P. Colombat, and H. Watier. 2002. Therapeutic activity of humanized anti-CD20 monoclonal antibody and polymorphism in IgG Fc receptor FcgammaRIIIa gene. *Blood* 99: 754–758.
26. Golay, J., E. Cittera, N. Di Gaetano, M. Manganini, M. Mosca, M. Nebuloni, N. van Rooijen, L. Vago, and M. Introna. 2006. The role of complement in the therapeutic activity of rituximab in a murine B lymphoma model homing in lymph nodes. *Haematologica* 91: 176–183.
27. Wang, S. Y., S. Veeramani, E. Racila, J. Cagley, D. C. Fritzinger, C. W. Vogel, W. St John, and G. J. Weiner. 2009. Depletion of the C3 component of complement enhances the ability of rituximab-coated target cells to activate human NK cells and improves the efficacy of monoclonal antibody therapy in an in vivo model. *Blood* 114: 5322–5330.
28. Gong, Q., Q. Ou, S. Ye, W. P. Lee, J. Cornelius, L. Diehl, W. Y. Lin, Z. Hu, Y. Lu, Y. Chen, et al. 2005. Importance of cellular microenvironment and circulatory dynamics in B cell immunotherapy. *J. Immunol.* 174: 817–826.
29. Golay, J., M. Lazzari, V. Facchinetti, S. Bernasconi, G. Borleri, T. Barbui, A. Rambaldi, and M. Introna. 2001. CD20 levels determine the in vitro susceptibility to rituximab and complement of B-cell chronic lymphocytic leukemia: further regulation by CD55 and CD59. *Blood* 98: 3383–3389.
30. McLaughlin, P., A. J. Grillo-López, B. K. Link, R. Levy, M. S. Czuczman, M. E. Williams, M. R. Heyman, I. Bence-Bruckler, C. A. White, F. Cabanillas, et al. 1998. Rituximab chimeric anti-CD20 monoclonal antibody therapy for relapsed indolent lymphoma: half of patients respond to a four-dose treatment program. *J. Clin. Oncol.* 16: 2825–2833.
31. Lindorfer, M. A., H. B. Jinivizian, P. L. Foley, A. D. Kennedy, M. D. Solga, and R. P. Taylor. 2003. B cell complement receptor 2 transfer reaction. *J. Immunol.* 170: 3671–3678.
32. Greenwood, J., M. Clark, and H. Waldmann. 1993. Structural motifs involved in human IgG antibody effector functions. *Eur. J. Immunol.* 23: 1098–1104.
33. Golay, J., M. Manganini, A. Rambaldi, and M. Introna. 2004. Effect of alemtuzumab on neoplastic B cells. *Haematologica* 89: 1476–1483.
34. Wang, Y. 2006. Complementary therapies for inflammation. *Nat. Biotechnol.* 24: 1224–1226.
35. Ivanov, A., S. A. Beers, C. A. Walshe, J. Honeychurch, W. Alduaij, K. L. Cox, K. N. Potter, S. Murray, C. H. Chan, T. Klymenko, et al. 2009. Monoclonal antibodies directed to CD20 and HLA-DR can elicit homotypic adhesion followed by lysosome-mediated cell death in human lymphoma and leukemia cells. *J. Clin. Invest.* 119: 2143–2159.
36. Golay, J., L. Bologna, P. A. André, F. Buchegger, J. P. Mach, L. Boumsell, and M. Introna. 2010. Possible misinterpretation of the mode of action of therapeutic antibodies in vitro: homotypic adhesion and flow cytometry result in artefactual direct cell death. *Blood* 116: 3372–3373, author reply 3373–3374.
37. Rebello, P., and G. Hale. 2002. Pharmacokinetics of CAMPATH-1H: assay development and validation. *J. Immunol. Methods* 260: 285–302.
38. Alter, G., J. M. Malenfant, and M. Altfeld. 2004. CD107a as a functional marker for the identification of natural killer cell activity. *J. Immunol. Methods* 294: 15–22.
39. Wang, S. Y., E. Racila, R. P. Taylor, and G. J. Weiner. 2008. NK-cell activation and antibody-dependent cellular cytotoxicity induced by rituximab-coated target cells is inhibited by the C3b component of complement. *Blood* 111: 1456–1463.
40. van der Kolk, L. E., A. J. Grillo-López, J. W. Baars, C. E. Hack, and M. H. van Oers. 2001. Complement activation plays a key role in the side-effects of rituximab treatment. *Br. J. Haematol.* 115: 807–811.
41. Kennedy, A. D., P. V. Beum, M. D. Solga, D. J. DiLillo, M. A. Lindorfer, C. E. Hess, J. J. Densmore, M. E. Williams, and R. P. Taylor. 2004. Rituximab infusion promotes rapid complement depletion and acute CD20 loss in chronic lymphocytic leukemia. *J. Immunol.* 172: 3280–3288.
42. Klepfish, A., L. Gilles, K. Ioannis, E. A. Rachmilewitz, and A. Schattner. 2009. Enhancing the action of rituximab in chronic lymphocytic leukemia by adding fresh frozen plasma: complement/rituximab interactions & clinical results in refractory CLL. [Published erratum appears in 2010 *Ann. N. Y. Acad. Sci.* 1204: 198.] *Ann. N. Y. Acad. Sci.* 1173: 865–873.
43. Taylor, R. P. 2008. Use of fresh frozen plasma to enhance the therapeutic action of rituximab. *QJM* 101: 991, author reply 991–992.
44. Zenz, T., M. Volden, T. Mast, A. Sarno, D. Winkler, A. Schnaiter, A. Buehler, C. Klein, P. Umana, H. Doehner, and S. Stilgenbauer. 2009. In vitro activity of the type II anti-CD20 antibody GA101 in refractory, genetic high-risk CLL. *ASH Ann. Meeting Abs.* 114: 939a.
45. Ashraf, S. Q., P. Umana, E. Mössner, T. Ntouroupi, P. Brünker, C. Schmidt, J. L. Wilding, N. J. Mortensen, and W. F. Bodmer. 2009. Humanised IgG1 antibody variants targeting membrane-bound carcinoembryonic antigen by antibody-dependent cellular cytotoxicity and phagocytosis. *Br. J. Cancer* 101: 1758–1768.

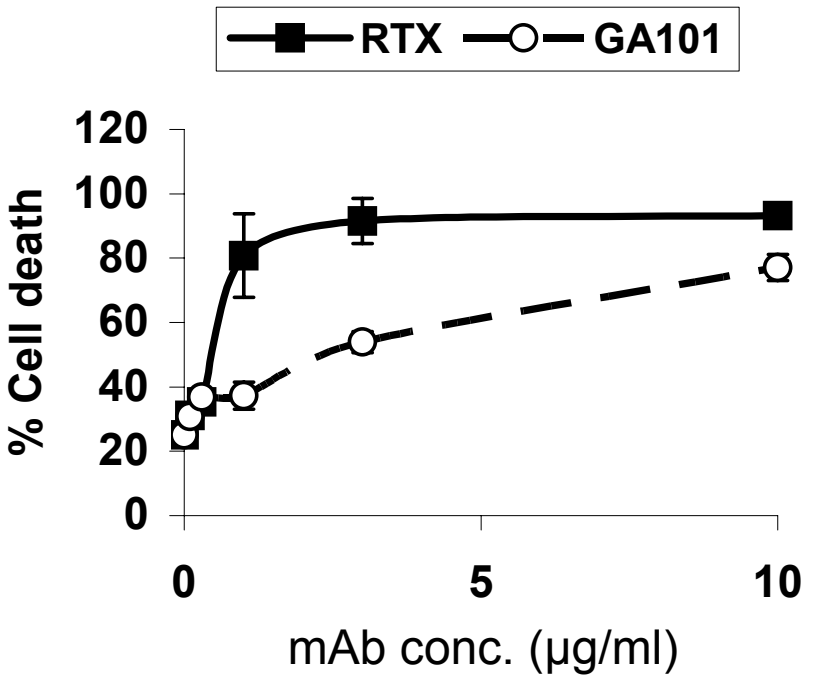

Supplementary Fig.1. Dose response of CDC activity of rituximab and GA101.

The DHL4 cell line was incubated with the indicated antibodies + 20% HS and cell death measured after 24 hours by 7AAD staining and FACS analysis.